modified N3′–>P5′ phosphoramidate DNA dodecamer duplex, J. Am. Chem. Soc. 120 (1998) 269–283.
[45] D. Barsky, M.E. Colvin, G. Zon, S.M. Gryaznov, Hydration effects on the duplex stability of phosphoramidate DNA-RNA oligomers, Nucleic Acids Res. 25 (1997) 830–835.
[46] N.K. Banavali, A.D. MacKerell, Re-examination of the intrinsic, dynamic and hydration properties of phosphoramidate DNA, Nucleic Acids Res. 29 (2001) 3219–3230.
[47] G. Zon, T.G. Geiser, Phosphorothioate oligonucleotides: chemistry, purification, analysis, scale-up and future directions, Anticancer Drug Des 6 (1991) 539–568.
[48] C.A. Stein, J.L. Tonkinson, L. Yakubov, Phosphorothioate oligodeoxynucleotides–anti-sense inhibitors of gene expression? Pharmacol. Ther. 52 (1991) 365–384.
[49] L. Xodo, M. Alunni-Fabbroni, G. Manzini, F. Quadrifoglio, Pyrimidine phosphorothioate oligonucleotides form triple-stranded helices and promote transcription inhibition, Nucleic Acids Res. 22 (1994) 3322–3330.

Molecules **2011**, *16*, 10695-10708; doi:10.3390/molecules161210695

OPEN ACCESS

molecules

ISSN 1420-3049

www.mdpi.com/journal/molecules

Article

Cleavage of Oligonucleotides Containing a P3'→N5' Phosphoramidate Linkage Mediated by Single-Stranded Oligonucleotide Templates

Kosuke Ramon Ito [1], Tetsuya Kodama [1], Futaba Makimura [1], Noritsugu Hosoki [1], Tomohisa Osaki [1], Ayako Orita [1,2], Takeshi Imanishi [1,2] and Satoshi Obika [1,*]

[1] Graduate School of Pharmaceutical Sciences, Osaka University, 1-6 Yamadaoka, Suita, Osaka 565-0871, Japan

[2] BNA Inc., 7-7-20 Saito-asagi, Ibaraki, Osaka 567-0085, Japan

* Author to whom correspondence should be addressed; E-Mail: obika@phs.osaka-u.ac.jp; Tel.: +81-6-6879-8200; Fax: +81-6-6879-8204.

Received: 1 November 2011; in revised form: 9 December 2011 / Accepted: 13 December 2011 / Published: 20 December 2011

Abstract: Double-stranded DNA (dsDNA) templates can hybridize to and accelerate cleavage of oligonucleotides containing a P3'→N5' phosphoramidate (P-N) linkage. This dsDNA-templated cleavage of P-N linkages could be due to conformational strain placed on the linkage upon triplex formation. To determine whether duplex formation also induced conformational strain, we examined the reactivity of the oligonucleotides with a P-N linkage in the presence of single-stranded templates, and compared these reactions to those with dsDNA templates. P-N oligonucleotides that are cleaved upon duplex formation could be used as probes to detect single-stranded nucleic acids.

Keywords: bridged nucleic acids; DNA sensing; P3'→N5' phosphoramidate

1. Introduction

Detection of nucleic acids via nucleic acid-templated reactions has attracted substantial interest [1-24]. Most of these techniques employ ligation of probes [1-11] and subsequent transfer [12-14], release [15-17], or activation [18-24] of a reporter group upon hybridization of the probes to the template DNA and/or RNA, based on an effective-molecularity approach [25]. When reactants are

placed in close proximity to template nucleic acids via sequence-specific hybridization, the effective molecularity of the reactants increases.

We presented a new type of DNA-templated reaction-based DNA detection; this method involves probe cleavage that is templated by double-stranded DNA (dsDNA) [26-29]. In this method, cleavage reactions are accelerated because of conformational strain induced by triplex formation, not because of the effective molecularity. We utilized triplex-forming oligonucleotides (TFOs) containing 5'-amino-2',4'-BNA (Figure 1, **X**) as probes; the TFOs have a P3'→N5' phosphoramidate (P-N) linkage in the backbone. This linkage was more susceptible to acid-mediated hydrolysis upon triplex formation, and the enhanced susceptibility was due to conformational strain on the P-N linkage induced by triplex formation. Previously, we examined the effects of chemical modifications that alter the microenvironment around the P-N linkage and change the extent of the conformational strain; these chemical modifications had substantial effects on the observed pseudo first-order rate constants (k_{obs}s) of the hydrolysis with the dsDNA templates [29]. These findings indicated that when the P-N linkage is subjected to sufficient strain, the linkage promptly breaks upon hybridization to the template. We hypothesized that duplex formation, like triplex formation, could induce conformational strain when oligonucleotides have a certain chemical modification and that such oligonucleotides may be selectively cleaved in the presence of single-stranded templates and, therefore, may be used as probes to detect single-stranded nucleic acids (Figure 2).

Here, we prepared several oligonucleotides containing a moiety (designated **X**, Figure 1) in the middle of a sequence with one of two chemical modifications, 2',4'-BNA/LNA [30-32] (designated **Y**) or 2',5'-linked DNA [33,34] (designated **L**), on adjacent residues (Table 1). The reactivity of these oligonucleotides in the presence of single-stranded DNA (ssDNA) or ssRNA templates was compared with their reactivity in the presence of parallel double-stranded DNA (**PDD**) templates and in the absence of any template. The parallel (Hoogsteen motif) single-stranded DNA and RNA (**PSD** and **PSR**, respectively) and anti-parallel (Watson-Crick motif) single-stranded DNA and RNA (**ASD** and **ASR**) were prepared as templates (see Table 1 caption). The formation of different motifs of duplexes was expected to have different effects on the reactivity of the hydrolysis depending on the extent of the strain.

Figure 1. Structures of **X** (5'-amino-2',4'-BNA), **Y** (2',4'-BNA/LNA), and **L** (2',5'-linked DNA).

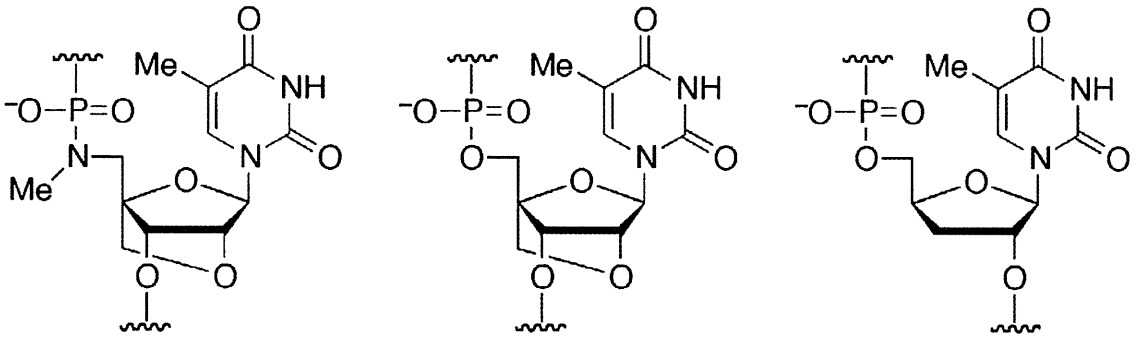

Figure 2. Schematic representation of nucleic acid-templated hydrolysis of phosphoramidate. Template nucleic acids can be dsDNA or parallel or anti-parallel single-stranded nucleic acids.

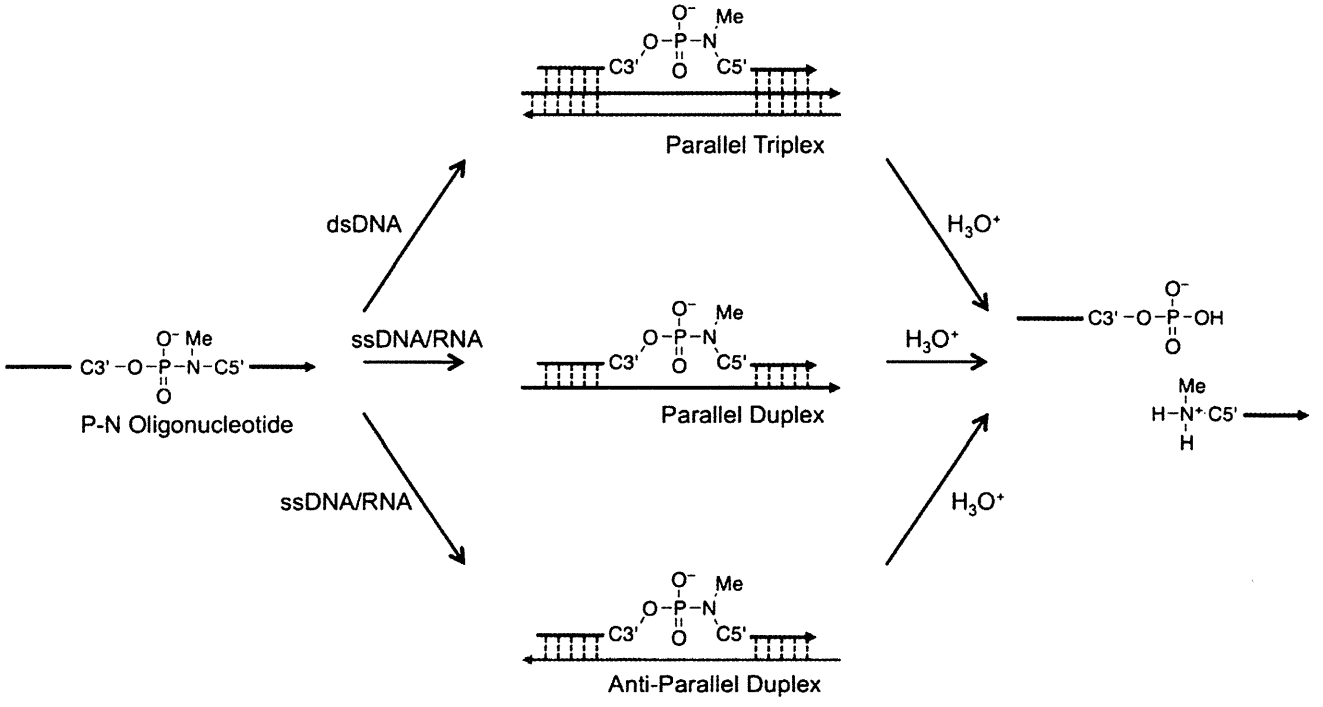

2. Results

2.1. UV Melting Experiments

Initially, we evaluated the ability of **ON-1**–**ON-8** to form duplexes with oligonucleotide templates. Although we tried to assess the affinity of **ON-1**–**ON-8** for template oligonucleotides under the acidic conditions in which the cleavage reactions were performed, it was not possible due to acid lability of **ON-1**–**ON-8** [29]. Therefore, we performed the melting experiments using **ON-0**, which has no P-N linkage, at pH 4.0 and under milder conditions (pH 6.0). The T_ms of **ON-0** at pH 6.0 and at pH 4.0 were compared with those of at pH 6.0 to estimate the stability of **ON-1**–**ON-8**-containing duplexes at pH 4.0. The T_m of each oligonucleotide is presented in Table 1, and the melting profiles are given in Figures 3 and S1.

The comparison between the heating and cooling processes provided information on hysteresis. Under slightly acidic conditions (pH 6.0), association and dissociation of **ON-0**–**ON-8** with parallel single-stranded RNA (**PSR**), anti-parallel single-stranded DNA (**ASD**) and RNA (**ASR**) were reversible, and no significant hysteresis was observed. In contrast, **ON-0**–**ON-8** showed hysteresis in the melting experiments with parallel single-stranded DNA (**PSD**). At pH 4.0, hysteresis was observed for duplexes **ON-0•PSD** and **ON-0•ASD**.

The effects of acidic conditions on the stability of the duplexes varied depending on the template. The duplex **ON-0•PSD** was stabilized at pH 4.0 (+15 °C), while the duplex **ON-0•PSR** was not stable under acidic conditions (T_m not determined). Anti-parallel duplexes were destabilized under acidic conditions, and the extent of the destabilization was much larger for the duplex **ON-0•ASR** (−18 °C) than that for **ON-0•ASD** (−4 °C).

Table 1. T_ms of duplexes containing an **ON-0–ON-8** oligonucleotide and **ASD**, **ASR**, **PSD**, or **PSR** [a].

ON	Sequence (5' to 3') [b]	T_m (ΔT_m) in °C with			
		PSD [c]	PSR [c]	ASD [c]	ASR [c]
ON-0	TTTTT^{m}CTTT^{m}CT^{m}CT^{m}CT	33 (-)	34 (-)	52 (-)	54 (-)
ON-0 [d]	TTTTT^{m}CTTT^{m}CT^{m}CT^{m}CT	48 (+15)	n.d. [e]	48 (−4)	36 (−18)
ON-1	TTTTT^{m}CTXT^{m}CT^{m}CT^{m}CT	38 (+5)	34 (±0)	54 (+2)	57 (+3)
ON-2	TTTTT^{m}CYXT^{m}CT^{m}CT^{m}CT	37 (+4)	37 (+3)	53 (+1)	60 (+6)
ON-3	TTTTT^{m}CTXY^{m}CT^{m}CT^{m}CT	41 (+8)	40 (+6)	55 (+3)	62 (+8)
ON-4	TTTTT^{m}CYXY^{m}CT^{m}CT^{m}CT	44 (+11)	44 (+10)	54 (+2)	65 (+11)
ON-5	TTTTY^{m}CTXT^{m}CY^{m}CT^{m}CT	45 (+12)	46 (+12)	57 (+5)	69 (+15)
ON-6	TTTTT^{m}CLXT^{m}CT^{m}CT^{m}CT	33 (±0)	34 (±0)	47 (−5)	55 (+1)
ON-7	TTTTT^{m}CTXL^{m}CT^{m}CT^{m}CT	31 (−2)	30 (−4)	49 (−3)	53 (−1)
ON-8	TTTTT^{m}CLXL^{m}CT^{m}CT^{m}CT	31 (−2)	29 (−5)	43 (−9)	51 (−3)

[a] Conditions: 140 mM KCl, 10 mM $MgCl_2$, 1.0 mM sodium phosphate, 10 mM sodium citrate, 1.5 μM each strand, pH 6.0; [b] **X**, 5'-amino-2',4'-BNA (NMe); **Y**, 2',4'-BNA/LNA; **L**, 2',5'-linked DNA; ^{m}C, 5-MedC; [c] **PSD** (parallel single-stranded DNA), 5'-d(AAAAAGAAAGAGAGA)-3'; **PSR** (parallel single-stranded RNA), 5'-r(AAAAAGAAAGAGAGA)-3'; **ASD** (anti-parallel single-stranded DNA), 5'-d(AGAGAGAAAGAAAAA)-3'; **ASR** (anti-parallel single-stranded RNA), 5'-r(AGAGAGAAAGAAAAA)-3'; [d] T_m measured at pH 4.0, for detail see experimental section; e: Not determined due to low stability (T_m < 25 °C).

Figure 3. Melting profiles of **ON-5** (left) and **ON-7** (right) with **PSD** (red, solid), **PSR** (red, dashed), **ASD** (blue, solid), and **ASR** (blue, dashed). Conditions: 140 mM KCl, 10 mM $MgCl_2$, 1.0 mM sodium phosphate, 10 mM sodium citrate buffer, 1.5 μM each strand, pH 6.0.

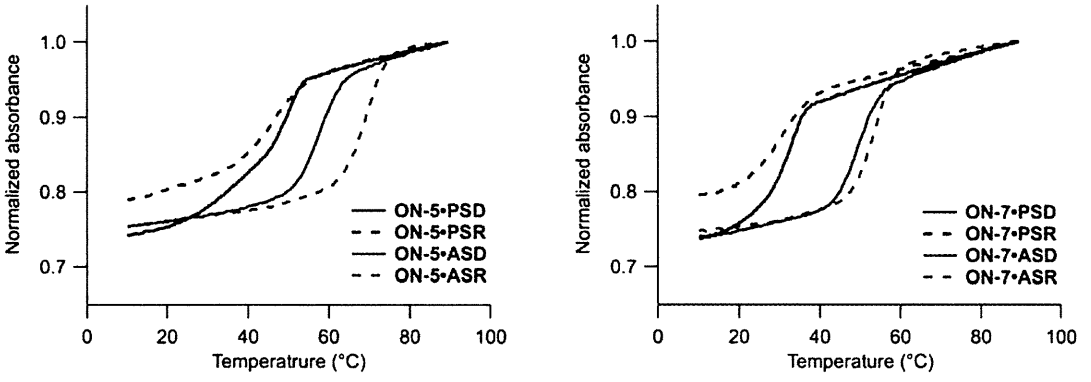

As we expected, introduction of 2',4'-BNA/LNA (**Y**) (**ON-2–ON-5**) stabilized the duplexes in most cases [30-32], and the stabilizing effects were more apparent for the duplexes with **PSD**, **PSR**, and **ASR** than those with **ASD**. Comparisons between **ON-2** and **ON-3** T_ms revealed that a **Y** positioned just 3' of **X** (5'-amino-2',4'-BNA) stabilized all duplexes to a larger extent than a **Y** positioned just 5' of **X**. Insertion of two residues between **X** and **Y** had greater stabilizing effects in all types of duplexes tested here (**ON-4** *vs.* **ON-5**). Comparison of T_ms of duplexes containing 2',5'-linked DNA (**L**) with those of **ON-1** revealed that introduction of **L** is destabilizing in most cases. The destabilization was less pronounced for the duplexes with **ASR**, as reported previously [35-37]. The melting curves of the duplexes consisting of **PSD** and **ON-3**, **ON-4**, or **ON-8** showed some two-transition character.

2.2. Hydrolysis Experiments

We performed hydrolysis experiments with **ON-1**–**ON-8** and single-stranded oligonucleotide templates (**PSD**, **ASD** and **ASR**) under conditions identical to those described previously for double-stranded DNA-templated reactions (pH 4.0, 40 °C), [28,29]. However, based on the duplex-forming ability of the oligonucleotides estimated from the UV melting experiments, the duplexes containing **ASR** were estimated to be destabilized under acidic conditions. Additionally, duplexes containing **PSD** did not exhibit sufficiently high thermal stability at pH 6.0, although they were estimated to be much more stable under acidic conditions. Therefore, the hydrolysis experiments using an **ON-1**–**ON-8** oligonucleotide and **ASR** or **PSD** were performed at 20 °C, because the duplexes were assumed to be sufficiently stable at this temperature. The duplexes with **PSR** were estimated to be significantly unstable under acidic conditions, and the reactivity on **PSR** was not evaluated. The k_{obs}s of each oligonucleotide at 40 °C and 20 °C are shown in Tables 2 and 3, respectively, and the cleavage profiles are shown in Figures 4, S2, S3 and S4.

Table 2. Observed pseudo first-order rate constants of each oligonucleotide at pH 4.0, 40 °C [a].

ON	$k_{obs} \times 10^3$ (s^{-1}) in the presence of				
	No template [b]	PDD [b,c]	PSD	ASD	ASR
ON-1	0.027 ± 0.005	0.77 ± 0.03	0.57 ± 0.09	0.14 ± 0.01	0.17 ± <0.01
ON-2	0.017 ± 0.006	0.051 ± 0.013	0.025 ± 0.001	0.020 ± 0.002	0.032 ± 0.001
ON-3	0.038 ± 0.012	1.4 ± 0.4	0.60 ± 0.05	0.10 ± <0.01	0.19 ± <0.01
ON-4	0.026 ± 0.003	0.044 ± 0.025	0.032 ± 0.003	0.015 ± 0.003	n.d. [d]
ON-5	0.029 ± 0.004	1.3 ± 0.4	0.86 ± 0.11	0.24 ± 0.02	0.19 ± <0.01
ON-6	0.066 ± 0.024	n.d. [d]	0.021 ± 0.004	0.021 ± 0.001	0.011 ± 0.001
ON-7	0.022 ± 0.002	2.1 ± 0.1	0.83 ± 0.03	0.29 ± <0.01	0.18 ± <0.01
ON-8	0.058 ± 0.003	0.022 ± 0.012	0.078 ± 0.003	0.035 ± 0.002	0.024 ± <0.001

[a] Conditions; 140 mM KCl, 10 mM $MgCl_2$, 1.0 mM sodium phosphate, 10 mM sodium citrate-HCl buffer, 3.35 μM each strand, pH 4.0, 40°C; [b] Taken from the previous reports [28,29]; [c] **PDD** (parallel double-stranded DNA); 5'-d(GCTAAAAAGAAAGAGAGATCG)-3'/ 5'-d(CGATCTCTCTTTCTTTTTAGC)-3'; [d] Not determined due to low reactivity.

Table 3. Observed pseudo first-order rate constants of each oligonucleotide at pH 4.0, 20 °C [a].

ON	$k_{obs} \times 10^3$ (s^{-1}) in the presence of		
	No template	PSD	ASR
ON-1	0.011 ± <0.001	0.27 ± 0.06	0.022 ± 0.001
ON-2	0.011 ± 0.002	0.0067 ± 0.0006	0.0059 ± 0.0006
ON-3	0.0072 ± 0.0010	0.19 ± 0.05	0.032 ± 0.002
ON-4	0.0062 ± 0.0011	n.d. [b]	n.d. [b]
ON-5	0.0073 ± 0.0015	0.26 ± 0.01	0.041 ± <0.001
ON-6	0.0067 ± 0.0013	n.d. [b]	n.d. [b]
ON-7	0.0080 ± 0.0008	0.68 ± 0.04	0.037 ± 0.005
ON-8	0.0070 ± 0.0005	n.d. [b]	n.d. [b]

[a] Conditions; see Table 2, the reaction temperature was 20 °C.; [b] Not determined due to low reactivity.

Figure 4. Cleavage profiles of **ON-7**, with no template (black, dashed), **PDD** (black, solid), **PSD** (red, solid), **ASD** (blue, solid), and **ASR** (blue, dashed) at pH 4.0, 40 °C. Black lines are drawn using the kinetic parameters given in Table 2.

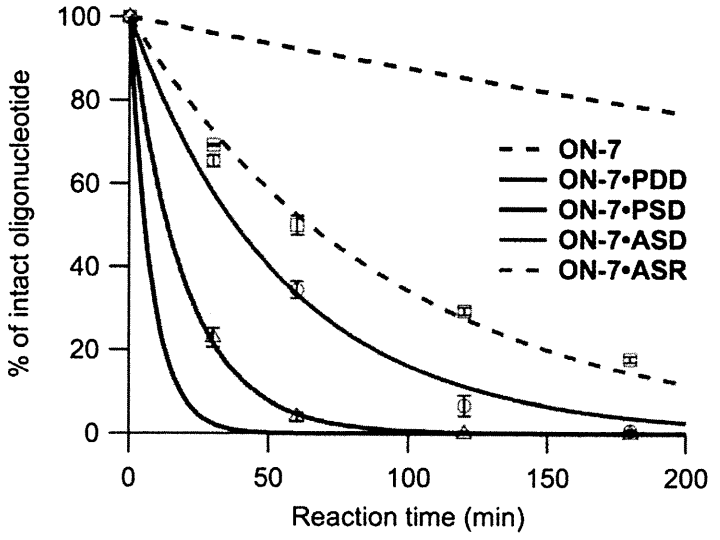

2.2.1. Reactivity on Parallel Single-Stranded DNA

The reactivity of **ON-1**–**ON-8** on **PSD** was similar to that on **PDD** (Table 2). The addition of **Y** to the 5'-neighboring residue of **X** (the sequence 5'-**YX**-3' found in **ON-2** and **ON-4**) resulted in inactivation of hydrolysis upon hybridization to **PSD** (Figure S2). **Y** added to the 3'-neighboring residue of **X** (5'-T**XY**-3') had little effect, resulting in equivalent k_{obs} for **ON-1** and **ON-3**. Accelerated hydrolysis of **ON-5** on **PSD** was observed as non-neighboring residual effects of **Y**. The sequence 5'-**LX**-3' found in **ON-6** and **ON-8** eliminated the acceleration associated with hybridization to **PSD**, while hydrolysis of **ON-7** (sequence 5'-T**XL**-3') was accelerated (Figure 4). At 20 °C, **ON-1**–**ON-8** were less reactive, but the reactivity of **ON-7** was least affected, and reactivities of **ON-1**, **ON-3**, and **ON-5** were equivalent in the presence of **PSD** (Table 3, Figure S3).

2.2.2. Reactivity on Anti-Parallel Single-Stranded DNA and RNA

In general, cleavage rate was lower in the presence of the anti-parallel single-stranded DNA or RNA than in the presence of **PDD** (Table 2). **ON-2**, **ON-4**, **ON-6**, and **ON-8** were not reactive in the presence of **ASD** or **ASR** (Figure S2). **ON-5** and **ON-7** were most reactive in the presence of **ASD**, but **ON-1**, **ON-3**, **ON-5**, and **ON-7** were all equally reactive in the presence of **ASR**. Although the reaction rate was slowed compared with that in the presence of **PDD**, **ON-7** showed 10 times higher reactivity in the presence of **ASD** than that in the absence of template (Figure 4). Lowering the reaction temperature to 20 °C resulted in significant decrease in reaction rate although the order of the reactivity was not affected (Table 3, Figure S3).

3. Discussion

Comparing the melting temperatures to the reactivities demonstrated that there seemed to be no direct correlation between the affinity to and reactivity on the templates. For examples, although **ON-3**

always showed higher affinity and reactivity on the templates than **ON-2**, the more reactive **ON-7** exhibited lower affinity to the templates than non-reactive **ON-6** in the reaction with **PSD** and **ASR**. The absence of direct relationships between T_m at pH 6.0 and k_{obs} at pH 4.0 was consistent with the previous finding on **PDD** [29]. Although we expected that the extent of the strain on the P-N linkage might be reflected as a change in the thermal stability of the duplexes and triplexes, it was difficult to extract information on the change in microenvironment around a P-N linkage from the overall thermal stability of complex.

We observed a difference between the reaction with **PSD** and **ASR** in terms of response to the change of reaction temperature. Although the lower reaction temperature (20 °C) always slowed the rate of reaction, the extent of decrease was different between the reactions on **PSD** and **ASR** templates. In the reaction with **ASR**, the relative rates (ratio of k_{obs} at 20 °C to k_{obs} at 40 °C; *i.e.*, for the reaction with **ON-1** and **ASR**, k_{obs} was 0.022 and 0.17 at 20 °C and 40 °C, respectively, and the relative rate was 13%) varied from 13% to 22% for **ON-1**, **ON-3**, **ON-5**, and **ON-7**, and they varied from 30% to 82% in the reactions with **PSD**. This difference may indicate the presence of a substantial amount of unbound oligonucleotides in the reaction with **PSD** at 40 °C. However, judging from the melting experiments, we can estimate that the thermal stability of the duplexes with **PSD** was higher than that with **ASR** at pH 4.0, and the unbound fractions, if present, should be larger in the reactions with **ASR**. Moreover, the cleavage profiles at 40 °C seemed to follow pseudo first-order kinetics for both the reactions with **PSD** and **ASR**, indicating that substantial amounts of unbound oligonucleotides were not present (Figure S2). Thus, we suppose that the difference in the relative rates between the reactions with **PSD** and **ASR** was not due to thermal stability of the duplexes, but the temperature dependency of the reaction. Temperature dependency of these reactions may have depended on the activation energy of the cleavage and/or the temperature dependency of basicity of phosphoramidates.

The lability of the P-N linkage in duplexes was affected by both chemical modifications in oligonucleotides and the motif of the duplexes. Similar reactivities were observed in the reactions with **PSD** and those with **PDD**; this similarity indicated that the microenvironment around the P-N linkage resembled each other. This finding was not surprising because **PSD** was designed to form Hoogsteen-type parallel duplexes, which are a component of the reaction with **PDD**. Based on CD and IR spectra, the structure of triplexes and Hoogsteen duplexes are reportedly similar [38]. In contrast, **PSR** showed completely different behavior. While it is well known that triplexes and Hoogsteen duplexes are stabilized under acidic conditions [32,39-41], the stability of duplex **PSR•ON-0** was significantly lowered at pH 4.0 (Table 1, Figure S1). The absence of hysteresis for duplexes containing **PSR** was observed, but hysteresis was observed when duplex contained **PSD**. Moreover, triplexes containing RNA as a purine strand and DNA as a third strand did not form even in acidic conditions [42-45]. Therefore, we assume that **PSR** did not form Hoogsteen-type duplexes and that the duplexes with **PSR** were unstable under acidic conditions. Thus, **PSR** were apparently not suitable templates for acid-mediated hydrolysis of the phosphoramidate, and the reactivity with **PSR** templates was not evaluated.

In the reactions with anti-parallel single-stranded DNA and RNA (**ASD** and **ASR**), the rate constants were as small as one-tenth of those in the reactions with **PDD**, indicating that the strain on the P-N linkage was not positioned appropriately. Recently, we proposed that the elevated basicity of the phosphoramidate may be responsible for accelerated hydrolysis [29]. From this point of view, the α

and ζ dihedral angles would be important because they should have a significant impact on the electronic state of the phosphoramidate (Figure 5).

Figure 5. Molecular model of the **ON-1•ASD** duplex. **ON-1** and **ASD** rendered as stick (colored by element) and space-filling (gray) models, respectively. α (O3'-P-N5'-C5') and ζ (C3'-O3'-P-N5').

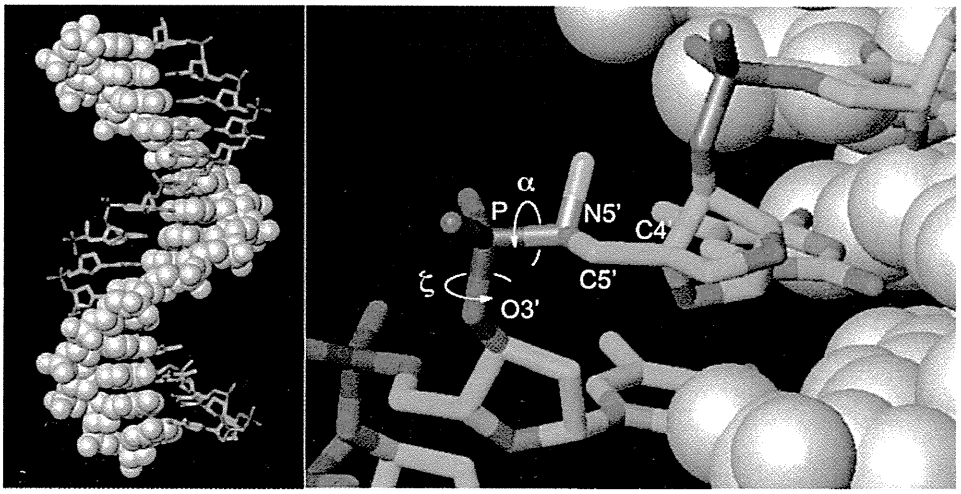

The duplexes containing **ASD** or **ASR** were likely to have B-form and A-form conformations [46], respectively, in which the α and ζ dihedral angles adopt *–sc* orientations [47]. The molecular models of **ON-1** with **ASD**, **ASR**, or **PDD** indicated that introduction of **X** did not prohibit α and ζ dihedral angles from adopting *–sc* orientations (Figure 5, S5). However, the high reactivity in triplexes and parallel Hoogsteen duplexes may have been due to a change in the preferred dihedral angles, which would make the phosphoramidates more basic. The quantum chemical calculations using one model compound (*N*,*N*,*O*-trimethylphosphoramidate, R = R' = Me in Scheme 1) revealed the relative stability between the neutral form (N-protonated) and the anionic form of the phosphoramidate (Scheme 1) as functions of α and ζ.

Scheme 1. Equilibrium between neutral and anionic form and hydrolysis of phosphoramidate.

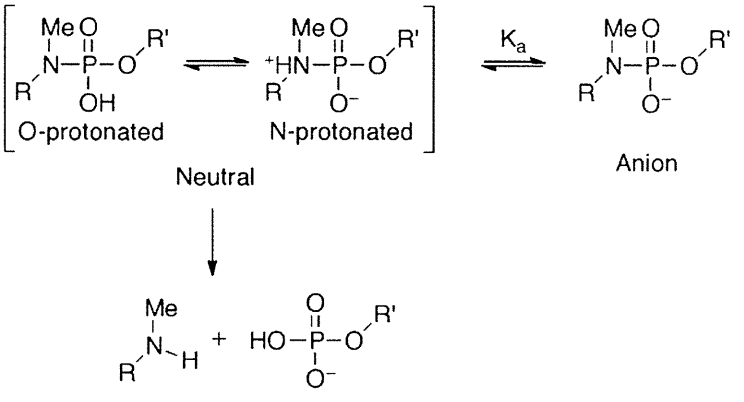

The N-protonated neutral form was considered to be the substrate in this reaction because the hydrolysis seemed to take place as a water molecule attacked from backside of the P-N linkage [28]. As is shown in Figure 6, the prevailing conformations in A- and B-form duplexes (α: −60°, ζ: −75°

A-form/−90° B-form [47]) were calculated to be relatively stable in the anionic form. Increment and decrement in α and ζ dihedral angles, respectively, will favor the electrically neutral form (Figure 6, C). Especially, the basicity of the phosphoramidate was estimated to be strongest when the α and ζ dihedral angles were −30° and −120° (Figure 6D), respectively, and such a conformation might be preferred in the triplex and parallel Hoogsteen duplex, resulting in enhanced reactivity.

Figure 6. Relative energy of phosphoramidate model compound as function of α and ζ dihedral angles. The relative energy was calculated from the minimized structure at density functional B3LYP/6-311+G** level of theory. The calculation was performed *in vacuo* with the two dihedral angles corresponding to α and ζ constrained to angles ranging from −120° to −30° in increment of 15°. The relative energy profiles of the neutral form (**A**) and anionic form (**B**) are shown. The N-protonated (zwitterionic) form was used as the neutral form. The difference in relative energy between anionic form and neutral form (**C**) was calculated by subtraction of relative energy of anion form (**B**) from that of neutral form (**A**). The most basic conformer studied here is shown (**D**; α and ζ were –30° and –120°, respectively). α: O3'-P-N5'-C5', ζ: C3'-O3'-P-N5'.

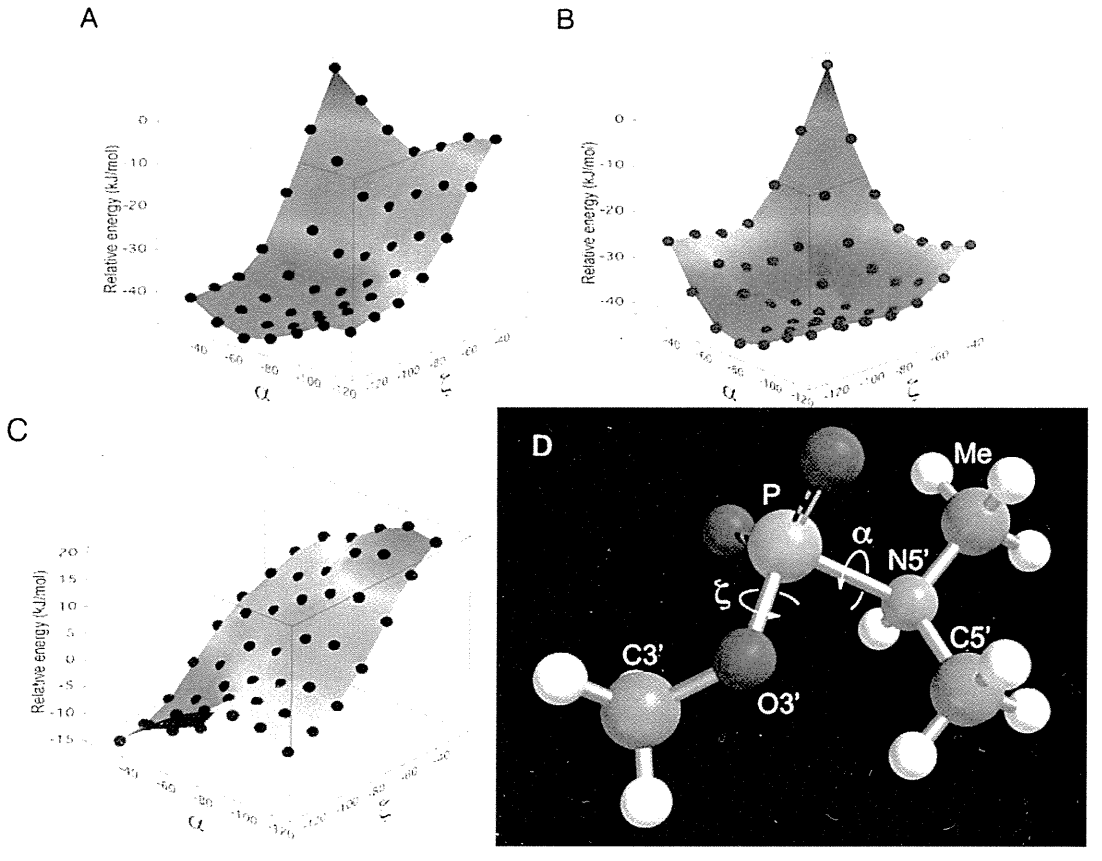

Although the structure of triplexes and parallel duplexes varies depending on the sequence and manner of determination [38,48,49], increased and decreased α and ζ dihedrals (α: −37° and ζ: −113°) are found in the model of parallel Hoogsteen duplex proposed by Sasisekharan *et al.* [38].

Our analysis of the effects of chemical modifications revealed that the orders of the reactivity of the oligonucleotides were nearly consistent regardless of the motifs of the duplexes. **ON-2**, **ON-4**, **ON-6,** and **ON-8** were always non-reactive, while **ON-5** and **ON-7** were the most reactive in the presence of

templates. It seemed that the microenvironment around the P-N linkage was, to an extent, conserved in the right-handed helical structures studied here. Although the prediction of the precise conformation requires further investigation, the effects of chemical modifications could also be explained by alteration of conformational preference. For example, **Y** is known to affect the sugar conformation of 3'-adjacent nucleotide inducing C3'-*endo* conformation [50,51]. Although such an effect is not the case in **ON-2** and **ON-4** because **X** is pre-locked to C3'-*endo* conformation due to the 2',4'-bridge moiety [26], **Y** at 5'-adjacent of the phosphoramidate will have structurally affected the preferred conformation of the phosphoramidate, which resulted in inactivation of **ON-2** and **ON-4** in the presence of templates.

4. Experimental Section

4.1. Preparation of Oligonucleotides

Natural oligonucleotides and those with 2'-deoxy-5-methylcytidine (5-MedC), such as the template DNA (**PSD**, **ASD**), RNA (**PSR**, **ASR**), and **ON-0**, were purchased from Hokkaido System Science Co., Ltd., Sapporo, Japan. Oligonucleotides containing 5'-amino-2',4'-BNA (**ON-1**–**ON-8**) were synthesized as described previously [29].

2.2. UV Melting Experiments

UV melting experiments were performed using Shimadzu UV-1650 and Shimadzu UV-1800 spectrometers. Oligonucleotides were dissolved in a solution buffered to pH 6.0 or 4.0 containing 140 mM KCl, 10 mM $MgCl_2$, 1.0 mM sodium phosphate, and 10 mM sodium citrate (pH 6.0) or 10 mM sodium citrate-HCl (pH 4.0). The final concentration of each oligonucleotide was 1.5 μM. Solutions containing the oligonucleotides were heated and subsequently cooled to 10 °C to generate duplexes. Each solution was heated and subsequently cooled from 10 °C to 90 °C to 10 °C at the rate of 0.5 °C/min, and the hyperchromic changes were monitored at 260 nm. The melting temperatures (T_ms) were determined as the intersection of the melting curve and the median of lower and higher base lines derived from the heating processes (Table 1, Figure 3, Figure S1).

4.3. Hydrolysis Experiments

Hydrolysis experiments were performed as described previously [28,29]. The reaction solutions contained 140 mM KCl, 10 mM $MgCl_2$, 1.0 mM sodium phosphate, 10 mM sodium citrate-HCl, and 3.35 μM of each strand. The final pH was 4.0. Reaction solutions were kept at 40 °C or 20 °C for 0, 30, 60, 120, and 180 min, and each reaction solution (10 μL) was diluted with 100 mM glycine-NaOH (pH 9.0, 160 μL). The diluted samples were analyzed by reversed-phase HPLC (Shimadzu Prominence LC-20 system, Kyoto, Japan) to determine the percent of intact oligonucleotides (Table 2, 3, Figure 4, Figure S2, S3, S4).

4.4. Molecular Modeling and Computation

The initial structures for molecular modeling, **ON-1•ASD**, **ON-1•ASR**, and **ON-1•PDD**, were generated with Discovery Studio 3.1™ (Accelrys Software, Inc., San Diego, CA, USA) using default parameters for B-form DNA•DNA duplexes, A-form DNA•RNA duplexes, and triplexes, respectively. In the initial models, **ON-1** contained 2',4'-BNA/LNA in place of **X**. The structures generated were exported to MacroModel 9.1™ (Schrödinger, LLC, New York, NY, USA). An energy minimization calculation was performed for each structure using 1) AMBER* as a force field, 2) the GB/SA solvation model of water, and 3) the PRCG method to obtain structures optimized to within a gradient of 0.05 kJ/molÅ. Finally, the 5'-oxygen of 2',4'-BNA/LNA in **ON-1** of the optimized structures was replaced by nitrogen attached to a methyl group to obtain the molecular models (Figure 5, Figure S5).

The quantum mechanical calculations were performed with Spartan'08 for Mac (Wavefunction, Inc., Irvine, CA, USA). The two dihedral angles of *N,N,O*-trimethylphosphoramidate corresponding to α and ζ were constrained to angles ranging from −120° to −30° in increments of 15°. The constrained structures were subject to geometric optimization at semi-empirical PM3, HF/6-31+G* and density functional B3LYP/6-311+G** level of theory. All calculations were performed *in vacuo* (Figure 6).

5. Conclusions

We demonstrated that duplex formation induced conformational strain on the P-N linkage in oligonucleotides. Parallel Hoogsteen duplex formation brought higher reactivity than Watson-Crick duplex formation. The introduction of 2',5'-linked DNA at the 3'-neighboring residue of 5'-amino-2',4'-BNA promoted high reactivity in the presence of parallel and anti-parallel single-stranded DNA, as well as with parallel dsDNA templates.

Supplementary Materials

Supplementary materials can be accessed at: http://www.mdpi.com/1420-3049/16/12/10695/s1.

Acknowledgments

K.R.I. thanks the Research Fellowship from the Japan Society for the Promotion of Science (JSPS) for Young Scientists.

Conflict of Interest

The authors declare no conflicts of interest.

References

1. Xu, Y.; Karalkar, N.B.; Kool, E.T. Nonenzymatic autoligation in direct three-color detection of RNA and DNA point mutations. *Nat. Biotechnol.* **2001**, *19*, 148-152.
2. Sando, S.; Kool, E.T. Quencher as leaving group: Efficient detection of DNA-joining reactions. *J. Am. Chem. Soc.* **2002**, *124*, 2096-2097.

3. Abe, H.; Kool, E.T. Destabilizing universal linkers for signal amplification in self-ligating probes for RNA. *J. Am. Chem. Soc.* **2004**, *126*, 13980-13986.
4. Ficht, S.; Dose, C.; Seitz, O. As fast and selective as enzymatic ligations: Unpaired nucleobases increase the selectivity of DNA-controlled native chemical PNA ligation. *ChemBioChem* **2005**, *6*, 2098-2103.
5. Dose, C.; Ficht, S.; Seitz, O. Reducing product inhibition in DNA-template-controlled ligation reactions. *Angew. Chem. Int. Ed.* **2006**, *45*, 5369-5373.
6. Abe, H.; Kool, E.T. Flow cytometric detection of specific RNAs in native human cells with quenched autoligating FRET probes. *Proc. Natl. Acad. Sci. USA* **2006**, *103*, 263-268.
7. Ogasawara, S.; Fujimoto, K. SNP genotyping by using photochemical ligation. *Angew. Chem. Int. Ed.* **2006**, *45*, 4512-4515.
8. Yoshimura, Y.; Noguchi, Y.; Sato, H.; Fujimoto, K. Template-directed DNA photoligation in rapid and selective detection of RNA point mutations. *ChemBioChem* **2006**, *7*, 598-601.
9. Peng, X.; Greenberg, M.M. Facile SNP detection using bifunctional, cross-linking oligonucleotide probes. *Nucleic Acids Res.* **2008**, *26*, e31.
10. Abe, H.; Kondo, Y.; Jinmei, H.; Abe, N.; Furukawa, K.; Uchiyama, A.; Tsuneda, S.; Aikawa, K.; Matsumoto, I.; Ito, Y. Rapid DNA chemical ligation for amplification of RNA and DNA signal. *Bioconjug. Chem.* **2008**, *19*, 327-333.
11. Dose, C.; Seitz, O. Single nucleotide specific detection of DNA by native chemical ligation of fluorescence labeled PNA-probes. *Bioorg. Med. Chem.* **2008**, *16*, 65-77.
12. Grossmann, T.N.; Seitz, O. DNA-catalyzed transfer of a reporter group. *J. Am. Chem. Soc.* **2006**, *128*, 15596-15597.
13. Grossmann, T.N.; Röglin, L.; Seitz, O. *Angew. Chem. Int. Ed.* **2008**, *47*, 7119-7123.
14. Grossmann, T.N.; Seitz, O. Nucleic acid templated reactions: Consequences of probe reactivity and readout strategy for amplified signaling and sequence selectivity. *Chem. Eur. J.* **2009**, *15*, 6723-6730.
15. Brunner, J.; Mokhir, A.; Kraemer, R. DNA-templated metal catalysis. *J. Am. Chem. Soc.* **2003**, *125*, 12410-12411.
16. Boll, I.; Krämer, R.; Brunner, J.; Mokhir, A.; Templated metal catalysis for single nucleotide specific DNA sequence detection. *J. Am. Chem. Soc.* **2005**, *127*, 7849-7856.
17. Franzini, R.M.; Kool, E.T. Efficient nucleic acid detection by templated reductive quencher release. *J. Am. Chem. Soc.* **2009**, *131*, 16021-16023.
18. Cai, J.; Li, X.; Yue, X.; Taylor, J.S. Nucleic acid-triggered fluorescent probe activation by the Staudinger reaction. *J. Am. Chem. Soc.* **2004**, *126*, 16324-16325.
19. Cai, J.; Li, X.; Taylor, J.S. Improved nucleic acid triggered probe activation through the use of a 5-thiomethyluracil peptide nucleic acid building block. *Org. Lett.* **2005**, *7*, 751-754.
20. Pianowski, Z.L.; Winssinger, N. Fluorescence-based detection of single nucleotide permutation in DNA via catalytically templated reaction. *Chem. Commun.* **2007**, 3820-3822.
21. Franzini, R.M.; Kool, E.T. 7-Azidomethoxy-coumarins as profluorophores for templated nucleic acid detection. *ChemBioChem* **2008**, *9*, 2981-2988.
22. Franzini, R.M.; Kool, E.T. Organometallic activation of a fluorogen for templated nucleic acid detection. *Org. Lett.* **2008**, *10*, 2935-2938.

23. Furukawa, K.; Abe, H.; Wang, J.; Uda, M.; Koshino, H.; Tsuneda, S.; Ito, Y. Reduction-triggered red fluorescent probes for dual-color detection of oligonucleotide sequences. *Org. Biomol. Chem.* **2009**, *7*, 671-677.
24. Prusty, D.K.; Herrmann, A. A fluorogenic reaction based on heavy-atom removal for ultrasensitive DNA detection. *J. Am. Chem. Soc.* **2010**, *132*, 12197-12199.
25. Li, X.; Liu, D.R. DNA-templated organic synthesis: Nature's strategy for controlling chemical reactivity applied to synthetic molecules. *Angew. Chem. Int. Ed.* **2004**, *43*, 4848-4870.
26. Obika, S.; Nakagawa, O.; Hiroto, A.; Hari, Y.; Imanishi, T. Synthesis and properties of a novel bridged nucleic acid with a P3'→N5' phosphoramidate linkage, 5'-amino-2',4'-BNA. *Chem. Commun.* **2003**, 2202-2203.
27. Obika, S.; Tomizu, M.; Negoro, Y.; Osakai, T.; Orita, A.; Ueyama, Y.; Nakagawa, O.; Imanishi, T. Acid-mediated cleavage of oligonucleotide P3'→N5' phosphoramidates triggered by sequence-specific triplex formation. *Nucleos. Nucleot. Nucleic Acids* **2007**, *26*, 893-896.
28. Obika, S.; Tomizu, M.; Negoro, Y.; Orita, A.; Nakagawa, O.; Imanishi, T. Double-stranded DNA-templated digestion triggered by triplex formation. *ChemBioChem* **2007**, *8*, 1924-1928.
29. Ito, K.R.; Kodama, T.; Tomizu, M.; Negoro, Y.; Orita, A.; Osaki, T.; Hosoki, N.; Tanaka, T.; Imanishi, T.; Obika, S. Double-stranded DNA-templated cleavage of oligonucleotides containing a P3'→N5' linkage triggered by triplex formation: The effects of chemical modifications and remarkable enhancement in reactivity. *Nucleic Acids Res.* **2010**, *38*, 7332-7342.
30. Obika, S.; Nanbu, D.; Hari, Y.; Andoh, J.; Morio, K.; Doi, T.; Imanishi, T. Stability and structural features of the duplexes containing nucleoside analogues with a fixed N-type conformation, 2'-*O*,4'-*C*-methyleneribonucleosides. *Tetrahedron Lett.* **1998**, *39*, 5401-5404.
31. Singh, S.K.; Nielsen, P.; Koshkin, A.A.; Wengel, J. LNA (locked nucleic acids): Synthesis and high-affinity nucleic acid recognition. *Chem. Commun.* **1998**, 455-456.
32. Bhattacharyya, J.; Maiti, S.; Muhuri, S.; Nakano, S.; Miyoshi, D.; Sugimoto, N. Effect of locked nucleic acid modifications on the thermal stability of noncanonical DNA structure. *Biochemistry* **2011**, *50*, 7414-7425.
33. Rizzo, C.J.; Dougherty, J.P.; Breslow, R. 3'-Deoxy-2'-phosphoramidites of adenosine and 5-methyluridine used for the solid phase synthesis of unnatural 3'-deoxy-2'-5''-oligonucleotides. *Tetrahedron Lett.* **1992**, *33*, 4129-4132.
34. Dougherty, J.P.; Rizzo, C.J.; Breslow, R. Oligodeoxynucleotides that contain 2',5'' linkages: Synthesis and hybridization properties. *J. Am. Chem. Soc.* **1992**, *114*, 6254-6255.
35. Giannaris, P.A.; Damha, M.J. Oligoribonucleotides containing 2',5'-phosphodiester linkages exhibit binding selectivity for 3',5'-RNA over 3',5'-ssDNA. *Nucleic Acids Res.* **1993**, *21*, 4742-4749.
36. Prakash, T.P.; Jung, K.; Switzer, C. RNA recognition by the 2'-structural isomer of DNA. *Chem. Commun.* **1996**, 1793-1794.
37. Sheppard, T.L.; Breslow, R.C. Selective binding of RNA, not DNA, by complementary 2',5'-linked DNA. *J. Am. Chem. Soc.* **1996**, *118*, 9810-9811.
38. Raghunathan, G.; Miles, H.T.; Sasisekharan, V. Parallel nucleic acid helices with Hoogsteen base pairing: Symmetry and structure. *Biopolymers* **1994**, *34*, 1573-1581.

39. Singleton, S.F.; Dervan, P.B. Influence of pH on the equilibrium association constants for oligodeoxyribonucleotide-directed triple helix formation at single DNAsites. *Biochemistry* **1992**, *31*, 10995-11003.
40. Hashem, G.M.; Wen, J.; Do, Q.; Gray, D.M. Evidence from CD spectra and melting temperatures for stable Hoogsteen-paired oligomer duplexes derived from DNA and hybrid triplexes. *Nucleic Acids Res.* **1999**, 3371-3379.
41. Sugimoto, N.; Wu, P.; Hara, H.; Kawamoto, Y. pH and cation effects on the properties of parallel pyrimidine motif DNA triplexes. *Biochemistry* **2001**, *40*, 9396-9405.
42. Roberts, R.W.; Crothers, D.M. Stability and properties of double and triple helices: Dramatic effects of RNA or DNA backbone composition. *Science* **1992**, *258*, 1463-1466.
43. Han, H.; Dervan, P.B. Sequence-specific recognition of double helical RNA and RNA•DNA by triple helix formation. *Proc. Natl. Acad. Sci. USA* **1993**, *90*, 3806-3810.
44. Escudé, C.; François, J.; Sun, J.; Ott, G.; Sprinzl, M.; Garestier, T.; Hélène, C. Stability of triple helices containing RNA and DNA strands: experimental and molecular modeling studies. *Nucleic Acids Res.* **1993**, *21*, 5547-5553.
45. Han, H.; Dervan, P.B. Different conformational families of pyrimidine•purine•pyrimidine triple helices depending on backbone composition. *Nucleic Acids Res.* **1994**, *22*, 2837-2844.
46. Xiong, Y.; Sundaralingam, M. Crystal structure and conformation of a DNA-RNA hybrid duplex with a polypurine RNA strand: d(TTCTTBr^{5}CTTC)-r(GAAGAAGAA). *Structure* **1998**, *6*, 1493-1501.
47. MacKerell, A.D., Jr. Contribution of the intrinsic mechanical energy of the phosphodiester linkage to the relative stability of the A, B_I, and B_{II} forms of duplex DNA. *J. Phys. Chem. B* **2009**, *113*, 3235-3244.
48. Bhaumik, S.R.; Chary, K.V.R.; Govil, G.; Liu, K.; Miles, H.T. A novel palindromic triple-stranded structure fromed by homopyrimidine dodecamer d-CTTCTCCTCTTC and homopurine hexamer d-GAAGAG. *Nucleic Acids Res.* **1998**, *26*, 2981-2988.
49. Rhee, S.; Han, Z.; Liu, K.; Miles, H.T.; Davies, D.R. Structure of a triple helical DNA with a triplex-duplex junction. *Biochemistry* **1999**, *38*, 16810-16815.
50. Petersen, M.; Nielsen, C.B.; Nielsen, K.E.; Jensen, G.A.; Bondensgaard, K.; Singh, S.K.; Rajwanshi, V.K.; Koshkin, A.A.; Dahl, B.M.; Wengel, J.; *et al.* The conformations of locked nucleic acids (LNA). *J. Mol. Recognit.* **2000**, *13*, 44-53.
51. Jensen, G.A.; Singh, S.K.; Kumar, R.; Wengel, J.; Jacobsen, J.P. A comparison of the solution structures of an LNA:DNA duplex and the unmodified DNA:DNA duplex. *J. Chem. Soc. Perkin Trans. 2* **2001**, 1224-1232.

Sample Availability: Not available.

JOC The Journal of Organic Chemistry

Featured Article

pubs.acs.org/joc

Synthesis and Properties of a Bridged Nucleic Acid with a Perhydro-1,2-oxazin-3-one Ring

Ajaya R. Shrestha, Yoshiyuki Hari, Aiko Yahara, Takashi Osawa, and Satoshi Obika*

Graduate School of Pharmaceutical Sciences, Osaka University, 1-6 Yamadaoka, Suita, Osaka, 565-0871, Japan

Supporting Information

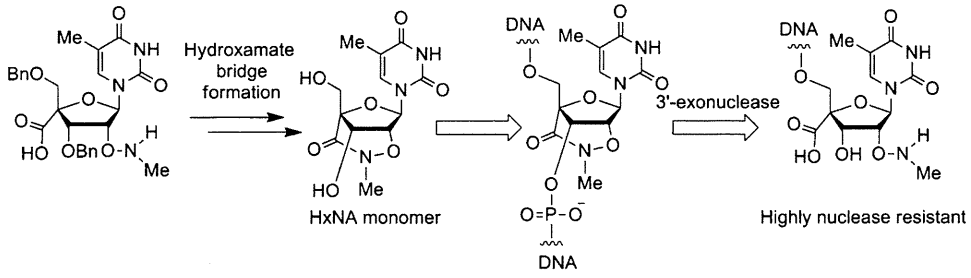

ABSTRACT: A novel derivative of 2′,4′-bridged nucleic acid, named hydroxamate-bridged nucleic acid (HxNA), containing a six-membered perhydro-1,2-oxazin-3-one ring, was designed and synthesized. The introduction of a carbonyl function along with an N−O linkage in the six-membered bridged structure is the unique structural feature of the novel 2′,4′-bridged nucleic acid analogue. The design was carried out to restrict the flexibility of the sugar moiety through the trigonal planarity of carbonyl function, which would improve the properties of the modification. The synthesized monomer was incorporated into oligonucleotides, and their properties were examined. The HxNA-modified oligonucleotides exhibited selectively high affinity toward complementary ssRNA. Furthermore, the nuclease resistance of the HxNA-modified oligonucleotide was found to be higher than that of the corresponding natural and 2′,4′-BNA/LNA-modified oligonucleotides. Interestingly, exposure of HxNA modified oligonucleotide to 3′-exonuclease resulted in gradual opening of the bridge, which stopped further digestion. Moreover, ring-opening of only one modification at the 3′-end of the oligonucleotides was observed, even if two or three HxNA modifications were present in the sequence. The results demonstrate the strong potential of the HxNA modification as a switch for the generation of highly nuclease-resistant RNA selective oligonucleotide in situ, which could have potential applications in antisense technology.

■ INTRODUCTION

The approach of using chemically modified nucleic acids for the selective control and regulation of gene expression has attracted much attention because of its potential for the development of highly potent therapeutics.[1−10] Conformationally restricted nucleic acids are one of the most interesting and promising candidates which could exhibit many of the desired properties of an ideal oligonucleotide.[11−15] It is well-known that a nucleic acid with its sugar conformation locked in *N*-type, termed 2′,4′-bridged nucleic acid (2′,4′-BNA),[16,17] or locked nucleic acid (LNA)[18] (**NA-1**, Figure 1) can exhibit unprecedented hybridizing affinity to complementary strands (RNA and DNA), sequence selectivity,[19] aqueous solubility, and potential for in vivo application.[20,21] On the basis of the structure of 2′,4′-BNA/LNA, many interesting modifications have been reported by other laboratories[22−26] and us[27,28] in the search for bridged nucleic acids with improved properties (Figure 1). It has been found that the properties of the 2′,4′-bridged nucleic acids are directly related to the size of the bridged structure and the heteroatom in the bridge. Increasing the size of the bridge, in general, increases the nuclease resistance at the expense of hybridizing affinity,[18,22,27] and the presence of heteroatom in the bridge apparently improves binding affinity.[22,25,27]

Recently, we have reported a modification with a six-membered bridged structure, 2′,4′-BNA^{NC}[27d] (**NA-2**), which exhibited interestingly high binding affinities toward ssRNA and dsDNA along with high nuclease resistance. 2′,4′-BNA^{NC} has the unique structural feature of N−O bond in the bridge of the six-membered ring system, which is attributable for the improved properties of the 2′,4′-BNA^{NC}-modified oligonucleotides. Very recently, we have developed another bridged nucleic acid with a seven-membered ring system having a cyclic urea structure (**NA-3**).[27e] The modification was developed to enhance the hydrophilicity of the modified oligonucleotide through the introduction of N−H and C=O groups in the structure as a proton donor and acceptor, respectively. The introduction of a carbonyl function in the bridge is an interesting approach for restricting the flexibility of the sugar conformation of a bridged nucleic acid with a larger ring system, which could result improved properties of the nucleic acid. In the case of the bridged nucleic acid with cyclic urea structure, highly RNA selective binding affinity was obtained along with promisingly high nuclease resistance.

Received: August 4, 2011
Published: November 7, 2011

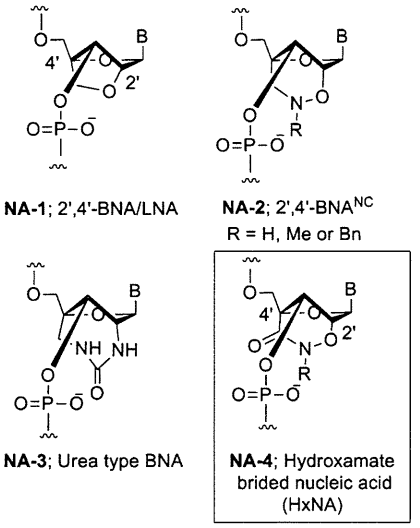

Figure 1. Structures of 2',4'-bridged nucleic acids.

We herein report the design, synthesis, and properties of a novel bridged nucleic acid analogue with a perhydro-1,2-oxazin-3-one ring system (**NA-4**). The modification was designed as a six-membered bridged structure with hydroxamate (N–O linkage and carbonyl function) moiety in the bridge. The design thus includes the important structural features of 2',4'-BNA^{NC} and the bridged nucleic acid with cyclic urea structure, which made it promising modification with potentially improved properties. We have accomplished the synthesis of the hydroxamate bridged nucleic acid (HxNA) with a thymine nucleobase, HxNA-T, using a condensation reaction between the aminooxy moiety at C2' and the carboxyl moiety at C4'. The synthesized HxNA was introduced into oligonucleotides, and their hybridizing affinities and nuclease resistance were investigated.

■ RESULTS AND DISCUSSION

Synthesis of HxNA. Considering the labile nature of N–O moiety, the construction of the bridge of the target monomer was strategically carried out at a late stage in the synthesis. Starting from the common precursor of 2',4'-BNA/LNA, i.e., 3-*O*-benzyl-4-*C*-hydroxymethyl-1,2-*O*-isopropylidene-α-D-ribofuranose **1**, the target monomers were synthesized in 14 and 16 synthetic steps. The regioselective benzylation of **1** afforded **2** in good yield.[18b,27d] The primary hydroxyl moiety of **2** was protected by silylation using TBDPSCl as a protecting agent to

Scheme 1[a]

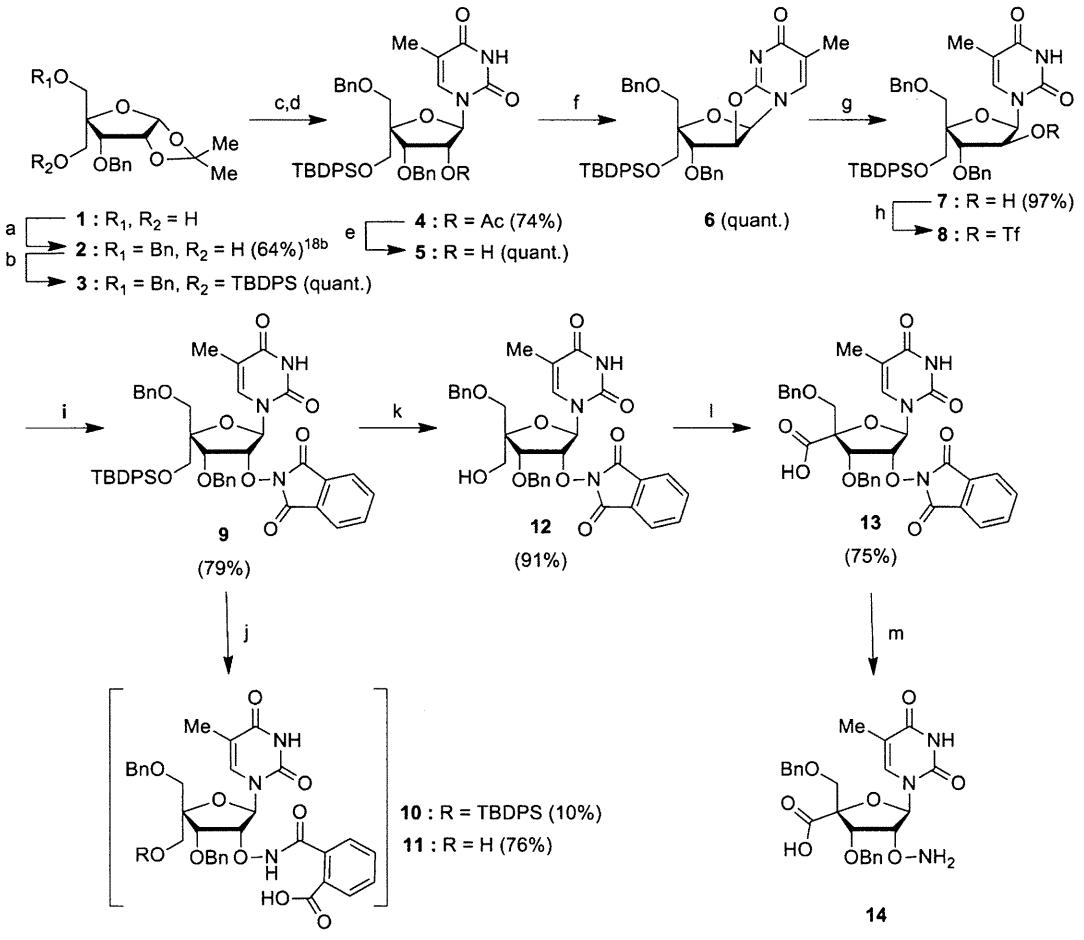

[a]Reagents and conditions: (a) NaH, BnBr, DMF, 0 °C to rt, 64%; (b) TBDPSCl, imidazole, DMF, rt, quant; (c) Ac_2O, concd H_2SO_4, AcOH, rt; (d) thymine, BSA, TMS-triflate, MeCN, reflux, 74% (two steps); (e) 40% $MeNH_2$ (aq), THF, rt, quant; (f) TfCl, DMAP, CH_2Cl_2, rt, quant; (g) 1 N NaOH (aq), THF, rt, 97%; (h) Tf_2O, pyridine, CH_2Cl_2, 0 °C; (i) *N*-hydroxyphthalimide, DBU, MeCN, rt 79%, two steps; (j) 1 N TBAF/THF, THF, reflux; (k) TEA·3HF, THF, reflux, 90%; (l) PDC/DMF, MS 4A, rt, 75%; (m) $NH_2NH_2{\cdot}H_2O$, EtOH, rt.

dx.doi.org/10.1021/jo201597e | J. Org. Chem. 2011, 76, 9891–9899

afford **3**. Acetolysis and acetylation of **3**, followed by stereoselective reaction with silylated thymine, afforded **4** in 74% yield. Subsequently, **4** was deacetylated by 40% methylamine to afford **5** in quantitative yield. The configuration of the 2′-carbon of **5** was successfully inverted to afford **7** in excellent yield by reacting **5** with TfCl to yield the 2,2′-anhydro derivative **6**, followed by alkaline hydrolysis. The N−O moiety was introduced into the structure by an S_N2 type substitution reaction with *N*-hydroxyphthalimide in presence of 1,8-diazabicyclo[5.4.0]undec-7-ene (DBU), yielding **9**. Desilylation of the TBDPS group was conducted using triethylamine trihydrofluoride (TEA·3HF) yielded **12** in excellent yield. It has been observed that the common desilylating agent, TBAF, was not appropriate because ring-opening reaction occurred at the base labile phthalimide moiety at 2′-position yielding **10** and **11**. Oxidation of the free hydroxyl moiety of **12** with PDC in DMF afforded the carboxylic acid **13** in good yield. Reaction of **13** with hydrazine monohydrate in ethanol yielded **14** with a free aminooxy moiety, which was used as the reactive key intermediate for the synthesis of the HxNA monomers (Scheme 1).

The aminooxy and carboxyl moieties of the key intermediate **14** were coupled using 1-ethyl-3-(3-dimethylaminopropyl)-carbodiimide hydrochloride (EDCI·HCl) in DMF as the coupling agent and hydroxybenzotriazole monohydrate (HOBt·H_2O) as the condensation additive to obtain the cyclized product **15**. The cyclized structure of **15** was confirmed by ^1H NMR spectroscopy where the 1′-H signal appeared as a singlet ($J_{1',2'}$ = 0 Hz), similar to 2′,4′-BNA/LNA, suggesting that the sugar moiety was in *N*-conformation.[16a] Debenzylation of **15** by catalytic hydrogenolysis with Pearlman's catalyst [20% Pd-$(OH)_2$/C] under a hydrogen atmosphere yielded the target nucleoside monomer **16** (Scheme 2). It is noteworthy that hydrogenolysis for debenzylation was not possible for the synthesis of 2′,4′-BNA^{NC}, as bond cleavage occurred at the N−O moiety,[27d] whereas the reaction occurred smoothly with no cleavage reaction in the case of HxNA, presumably due to the electron-withdrawing effect of the carbonyl function toward the N−O moiety.

Starting from the key intermediate **14**, the synthesis of the *N*-methyl congener of HxNA was accomplished in four consecutive steps (Scheme 2). The free aminooxy moiety of the key intermediate **7** was methylated by reductive amination; reacting **14** with formaldehyde yielded the imine **17** which was reduced by sodium cyanoborohydride in the presence of pyridinium *p*-toluenesulfonate to afford **18**. Cyclization of **18**, employing the coupling agent EDCI·HCl in DMF in the presence of HOBt·H_2O, yielded the product **19**. Debenzylation of **19** by catalytic hydrogenolysis afforded the target nucleoside monomer **20**.

The [NH] derivative of HxNA, having an unsubstituted nitrogen in the bridge, was found to be less stable under basic conditions, and it was difficult to synthesize desired phosphoramidite monomer of the derivative. Therefore, we have used the *N*-substituted HxNA, i.e., HxNA[NMe], for the preparation of modified oligonucleotides in this study. The synthesized HxNA monomer was incorporated into oligonucleotides using the standard phosphoramidite protocol except for a prolonged coupling time of 30−45 min with 5-[3,5-bis(trifluoromethyl)phenyl]-1*H*-tetrazole (Activator 42: Act42) as an activator. For the synthesis of the desired phosphoramidite **22**, the primary hydroxyl group of the nucleoside **20** was selectively protected with the 4,4′-dimethoxytrityl (DMTr) group to give **21**. The secondary hydroxyl group was then phosphitylated with 2-cyanoethyl *N,N,N′,N′*-tetraisopropylphosphorodiamidite to yield the HxNA[NMe]-thymine phosphoramidite **22** as a mixture of two diastereoisomers (Scheme 3).

Scheme 2[a]

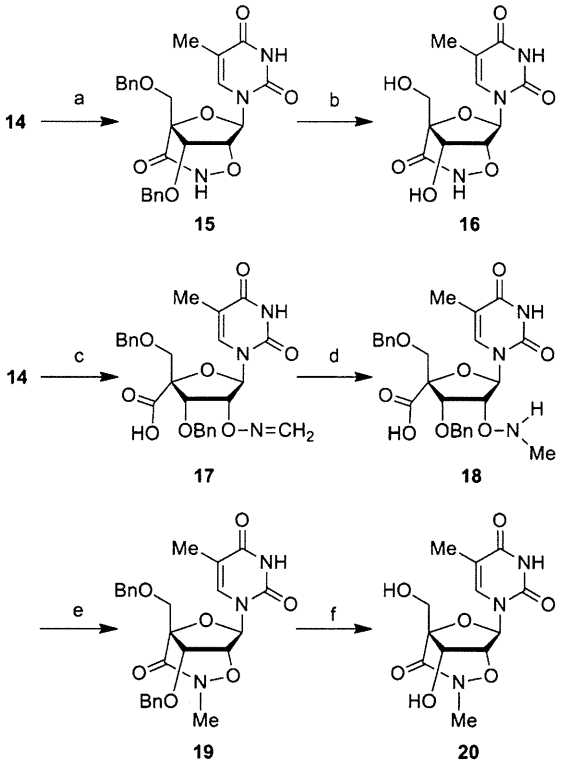

[a]Reagents and conditions: (a) EDCI·HCl, HOBt·H_2O, DMF, 77%, two steps; (b) H_2, Pd$(OH)_2$/C, EtOH/$CHCl_3$, 96%; (c) HCHO, MeOH, rt, 65%, two steps; (d) $NaBH_3CN$/1 M PPTS, MeOH, rt; (e) EDCI·HCl, HOBt·H_2O, DMF, rt, 80%, two steps; (f) H_2, Pd$(OH)_2$/C, EtOH/$CHCl_3$, rt, 90%.

Scheme 3[a]

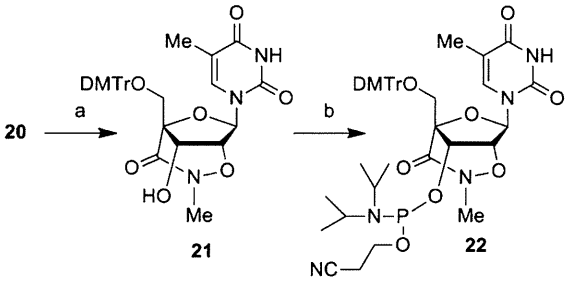

[a]Reagents and conditions: (a) DMTrCl, TEA, pyridine, rt, 60%; (b) 2-cyanoethyl *N,N,N′,N′*-tetraisopropyl phosphorodiamidite, 4,5-dicyanoimidazole, MeCN, rt, 70%.

During postsynthetic processing, it was found that ammonia treatment for deprotection and removal of oligonucleotides from the solid support was not possible because of ammonolytic cleavage of the bridge. Therefore, the synthesized oligonucleotides were treated with 50 mM potassium carbonate in methanol to obtain the desired oligonucleotide without any bond cleavage. The oligonucleotides were purified by reversed-phase HPLC (RP-HPLC) and characterized by MALDI-TOF

dx.doi.org/10.1021/jo201597e | *J. Org. Chem.* 2011, 76, 9891–9899

Table 1. T_m (°C) Values of Duplex Formed by HxNA-Modified Oligonucleotides with Complementary ssRNA and ssDNA[a]

	complementary RNA	complementary DNA	RNA selectivity
oligonucleotides	T_m (ΔT_m/mod) (°C)	T_m (ΔT_m/mod) (°C)	$\Delta T_{m(ssRNA-ssDNA)}$ (°C)
5′-d(TTTTTTTTTT)-3′ (**23**)	18	19	−1
5′-d(TTTTTXTTTT)-3′ (**24**)[b]	20 (+2)	12 (−7)	+8
5′-d(TTTXTXTTTT)-3′ (**25**)	24 (+3)	14 (−2.5)	+10
5′-d(TTTXTXTXTT)-3′ (**26**)	29 (+3.7)	21 (+0.7)	+8

[a]Target ssRNA: 5′-r(AAAAAAAAAA)-3′(**32**). Target ssDNA: 5′-d(AAAAAAAAAA)-3′(**33**). Conditions: 10 mM sodium phosphate buffer (pH 7.2) containing 100 mM NaCl; strand concentration = 4 μM. [b]T_m values of **24**/5′-r(AAAACAAAAA)-3′ and **24**/5′-r(AAAAUAAAAA)-3′were less than 10 °C.

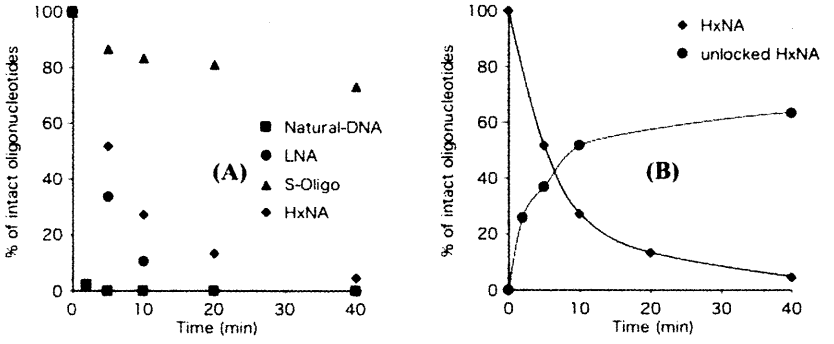

Figure 2. (A) Nuclease resistance of 5′-d(TTTTTTTTXT)-3′ against CAVP. X = HxNA (maroon solid diamond) (**27a**); natural DNA-T (red solid square) (**23**); 2′,4′-BNA/LNA-T (green solid circle) (**27b**); phosphorothioate-T (blue solid triangle) (**27c**). Experiments were performed at 37 °C in 100 μL of buffer containing 50 mM Tris-HCl (pH 8.0), 10 mM $MgCl_2$, CAVP (0.175 μg), and 7.5 μM of oligonucleotide. (B) Nuclease resistance of **27a** with HxNA modified singly at 2nd position from the 3′-end. The T-10 mer **27a** (maroon solid diamond) gradually degraded to the $n-1$ fragment from the 3′-end, the bridge of the HxNA modification opened, and the resulting T-9 mer (green solid circle) was highly stable toward nuclease degradation.

mass spectroscopy (mass spectral data and yields of the oligonucleotides are provided in the Supporting Information).

Thermal Stability of the Duplex Formed by HxNA. The thermal stability of the duplex formed by HxNA with complementary RNA, r(A_{10}) (**32**), and single-stranded DNA, d(A_{10}) (**33**), was monitored by UV melting experiments (T_m experiments). The results were compared with those obtained with natural d(T_{10}) oligonucleotide (**23**) and summarized in Table 1. The T_m value of the duplex formed between r(A_{10}) and singly modified oligonucleotide (**24**) was 2 °C higher than compared to that of natural d(T_{10})/r(A_{10}) duplex. An increase in the number of modifications increased the T_m value. For doubly (**25**) and triply (**26**) modified oligonucleotides, the increase in T_m was +3 and +3.7 °C per modification, respectively. In summary, the increase in T_m value per modification (ΔT_m/mod) of the HxNA ranged from 2.0 to 3.7 °C. Thus, the RNA binding affinity of HxNA was sufficiently higher than that of natural oligonucleotide and comparable to that of ENA;[22] however, it was lower than that of 2′,4′-BNA^{NC27d} (Table SI-3, Supporting Information). As regards RNA binding affinity, the effect of the hydroxamate bridge in HxNA was limited and less than what we expected in this case. In the case of duplex formation with complementary 10-mer DNA [d(A_{10})] the T_m values for singly (**24**) and doubly (**25**) modified oligonucleotides decreased by 7 and 2.5 °C per modification, respectively. Increasing the number of modifications to three (**26**) increased the T_m value to 0.7 °C per modification compared to the natural oligonucleotide.

Thus, the HxNA-modified oligonucleotides exhibited very high selectivitiy toward RNA similar to the urea-type bridged nucleic acid,[27e] indicating that introduction of a carbonyl function may help increase RNA selectivity of the bridged nucleic acid modified oligonucleotides. The T_m value of the duplex formed by singly modified HxNA oligonucleotide (**24**) with complementary ssRNA was +8 °C higher than that obtained with complementary ssDNA. The difference in T_m value increased to +10 °C when the oligonucleotide was modified doubly with HxNA (**25**) and +8 °C higher in the case of triply modified oligonucleotide (**26**) (Table 1). This result showed that the RNA selectivity of HxNA was more or less constant, in contrast with the urea-type bridged nucleic acid where the RNA selectivity increased as the number of modifications increased.[27e]

Nuclease Resistance of HxNA. The resistance of oligonucleotides modified with HxNA toward 3′-exonuclease (*Crotalus adamanteus* venom phosphodiesterase, CAVP, Pharmacia) was examined and compared with that of natural oligonucleotide, 2′,4′-BNA/LNA, and phosphorothioate (PS)-modified oligonucleotides, respectively. All of the oligonucleotides used in this study were 10-mers; those bearing modifications were modified singly at the second position from the 3′-end. The 10-mer HxNA-modified oligonucleotide (**27a**) was found to be less resistant to enzymatic degradation than the PS-modified oligonucleotide (**27c**) but exhibited better resistance than 2′,4′-BNA/LNA (**27b**) and natural d(T_{10}) oligonucleotide (**23**) (Figure 2A).

Interestingly, following the enzymatic removal of the first nucleotide, enzymatic digestion completely stopped. The progress of the enzymatic reaction was monitored by RP-HPLC; as the peak of **27a**, [5′-d(TTTTTTTTXT)-3′, where X = HxNA[NMe]-T], slowly diminished in size (peak **A**) a new peak (peak **B**) appeared and increased in size. The intensity of peak **B** increased with reaction time, and no other peaks appeared except **C** which is the peak of the T_1 monomer

(Figure 2B and 3). This result showed the high resistance of the degraded oligomer **28** toward enzymatic digestion. The

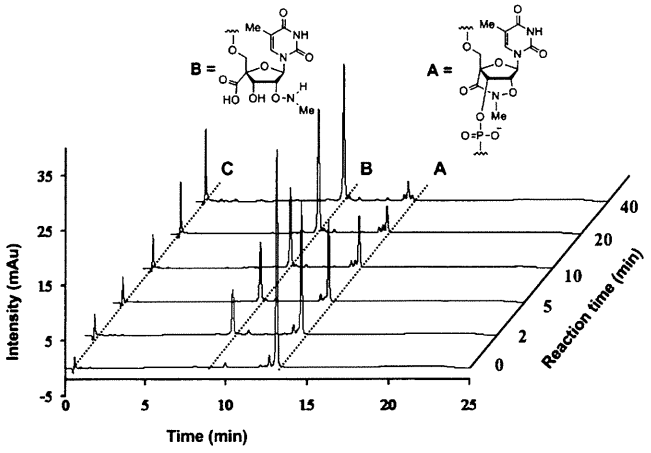

Figure 3. HPLC profile of the enzymatic degradation of HxNA-modified oligonucleotide **27a** with respect to time. Column: XBridge RP18 (3.0 × 50 mm). Mobile phase: Linear gradient of CH_3CN (7 to 14% over 20 min) in 0.1 M triethylammonium acetate (pH 7.0). Flow rate: 0.8 mL/min. Detection: absorbance at 260 nm.

degraded oligomers were isolated by RP-HPLC, and analyzed by MALDI-TOF mass spectrometry. Mass analysis confirmed that the degraded fragment **28** was the 9-mer oligonucleotide, but the bridged structure of the modification opened (Figure SI-43, Supporting Information). To check whether the buffer solution contributed to the ring-cleavage reaction, $dT_8\mathbf{X}T$ HxNA-modified oligonucleotide (**27a**) was incubated in the buffer solution for same length of time as in the enzymatic degradation experiment (40 min). This control experiment confirmed that the buffer solution played no role in either the degradation or the ring-opening of the modification.

The nuclease digestion experiment was conducted on three other 10-mer HxNA-modified oligonucleotides: modified singly at the fifth position [5′-d(TTTTTXTTTT)-3′ (**24**)], doubly at the fifth and seventh positions [5′-d(TTTXTXTTTT)-3′ (**25**)], and triply at the third, fifth, and seventh positions [5′-d(TTTXTXTXTT)-3′ (**26**)] from their 3′-end. In the case of the singly modified oligomer **24**, enzymatic digestion continued up to the fifth position from the 3′-end, as evidenced by the appearance of five peaks in the RP-HPLC profile. The fifth peak of these peaks, peak **B**, intensified with respect to time. Isolation and analysis (Figure SI-44, Supporting Information) of the degraded oligomer confirmed that the sequence of the highly nuclease resistant oligomer fragment was **29** [5′-d(TTTTTX′)-3′, where X′ = unlocked HxNA] with the ring of the modification opened. This result suggested that the HxNA modification has potential for generating highly nuclease-resistant oligomers in situ of the enzymatic reaction. If the enzyme cleaves only the modified moiety located at the extreme 3′-end of an oligonucleotide with multiple HxNA modifications, the modification could be developed into a switch to generate highly nuclease-resistant RNA selective oligonucleotides. To study the effect of the enzyme on the HxNA modification at positions other than the 3′-end, doubly (**25**) and triply (**26**) modified oligonucleotides were exposed to the 3′-exonuclease. As expected, degradation stopped at the first modified site from the 3′-end of both **25** and **26**, after opening of the modification, similar to the results of the previous experiments. Gratifyingly, no further digestion was observed, and the remaining modifications were not affected by the nuclease. MALDI-TOF mass analysis confirmed that the rest of the bridged structures remained intact (Figure SI-45 and Figure SI-46, Supporting Information). The HPLC profiles obtained during these experiments are shown in Figures SI-36–SI-38 in the Supporting Information. The MALDI-TOF masses of the degraded oligonucleotides with an unlocked HxNA modification are summarized in Table SI-2 in the Supporting Information. These results demonstrate the significant potential of the HxNA modification to act as a switch for generating highly nuclease-resistant monomer in situ of the enzymatic reaction, which may have interesting applications in the development of antisense oligonucleotides.

■ CONCLUSION

We have designed and synthesized a novel 2′,4′-bridged nucleic acid, HxNA, which contains a six-membered perhydro-1,2-oxazin-3-one ring system. The synthesis was accomplished in 14 and 16 synthetic steps using a condensation reaction between an aminooxy and a carboxyl moiety to close the ring. The synthesized HxNA[NMe]-T monomer was incorporated into oligonucleotides, and their properties were investigated. The HxNA[NH] monomer was not used in this study because of its instability under basic conditions and the difficulty of synthesizing its phosphoramidite derivative. The HxNA[NMe]-modified oligonucleotides exhibited highly selective hybridizing affinity toward complementary ssRNA with an increase in T_m values of 2–3.7 °C per modification. The nuclease resistance of HxNA-modified oligomer was higher than that of 2′,4′-BNA/LNA. Most interestingly, oligomers containing the unlocked derivative of the modification were found to be highly resistant toward enzymatic digestion: exposure of the HxNA-modified oligonucleotide to nuclease resulted in opening of the ring, with the ring-opened derivative resisting further degradation. Furthermore, only the modification located at the extreme 3′-end was affected by the nuclease; the other modifications remained unaffected. Thus, this modification has considerable potential to be developed into an in situ switch for generating highly nuclease-resistant antisense oligonucleotides with high RNA selectivity.

■ EXPERIMENTAL SECTION

General Methods. All moisture-sensitive reactions were carried out in well-dried glassware under a N_2 atmosphere. Anhydrous dichloromethane, DMF, MeCN, and pyridine were used as purchased. ^1H NMR spectra were recorded at 300 and 400 MHz, ^{13}C NMR were recorded at 75 and 100 MHz, and the ^{31}P spectrum was recorded at 161 MHz. Chemical shift values are expressed in δ values (ppm) relative to tetramethylsilane (TMS) as internal standard and residual solvents for ^1H NMR, and $CHCl_3$ (δ = 77.00 ppm), methanol (δ = 49.00 ppm), and DMSO (39.50 ppm) for ^{13}C NMR, and 85% H_3PO_4 (δ = 0 ppm) for ^{31}P NMR. Fast atom bombardment mass spectra (FAB-MS) were recorded in positive-ion mode. For column chromatography, silica gel PSQ 100B was used. The progress of the reaction was monitored by analytical thin-layer chromatography (TLC) on precoated aluminum sheets.

3,5-Di-O-benzyl-4-C-tert-butyldiphenylsiloxymethyl-1,2-O-isopropylidene-α-D-ribofuranose (3). To a solution of compound **2** (15.0 g, 37.4 mmol) in DMF (150 mL) were added imidazole (5.8 g, 85.1 mmol) and TBDPSCl (15.0 mL, 57.3 mmol) at 0 °C and the mixture stirred for 15 h at room temperature. After completion of the reaction, ice–water was added, and the product was extracted with diethyl ether. The organic phase was washed with water and brine solution and dried (Na_2SO_4). The product was purified by column

dx.doi.org/10.1021/jo201597e | J. Org. Chem. 2011, 76, 9891–9899